Supporting Information

Preparation and properties of novel $(Tb_{1-x}Ce_x)Sc_2Al_3O_{12}$ magneto-optical ceramics with different doping concentrations

Fang Wang[a,b], Yiheng Wu[b,d], Xieming Xu[b,d], Rui Zhang[a,b], Qi Luo[a,b], Hao Lu[b,d], Shuaihua Wang*[b,c], Shaofan Wu*[b,c]

[a]*College of Chemistry and Materials Science, Fujian Normal University, Fuzhou, Fujian 350117, China.*

[b]*Key Laboratory of Optoelectronic Materials Chemistry and Physics, Fujian Institute of Research on the Structure of Matter, Chinese Academy of Sciences, Fuzhou 350002, China.*

[c]*Fujian Science & Technology Innovation Laboratory for Optoelectronic Information of China, Fuzhou, Fujian 350108, China.*

[d]*University of Chinese Academy of Sciences, Beijing 100039, China.*

* E-mail: shwang@fjirsm.ac.cn.
sfwu@fjirsm.ac.cn

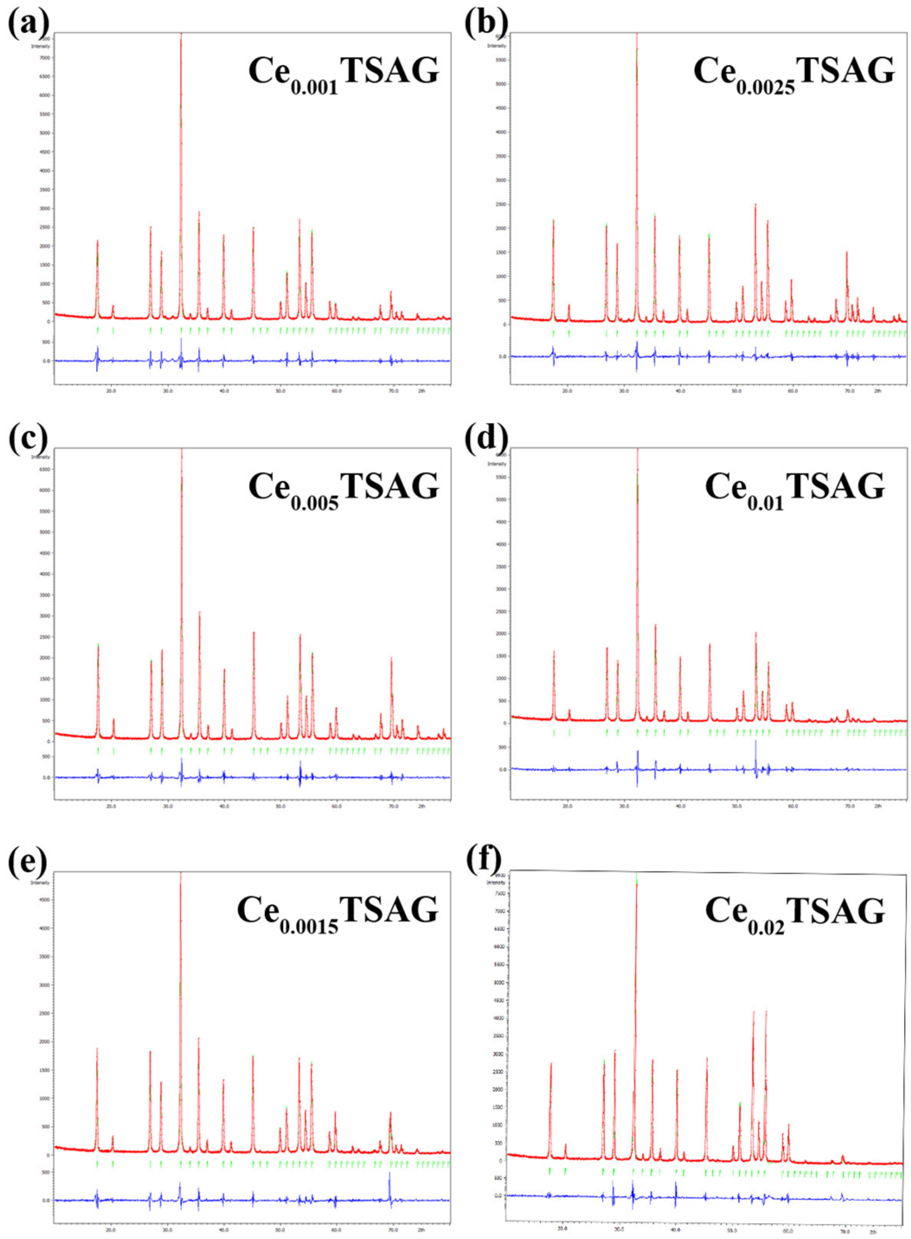

Figure S1. Rietveld refinement of $(Tb_{1-x}Ce_x)_3Sc_2Al_3O_{12}$ ceramics. (a) $Ce_{0.001}$TSAG. (b) $Ce_{0.0025}$TSAG. (c) $Ce_{0.005}$TSAG. (d) $Ce_{0.01}$TSAG. (e) $Ce_{0.0015}$TSAG. (f) $Ce_{0.02}$TSAG.

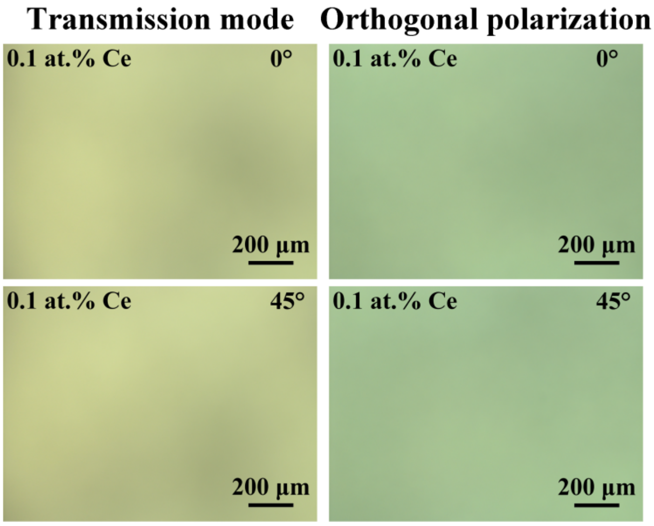

Figure S2. Transmission polarized optical microscopic images of the $Ce_{0.001}$TSAG ceramic (The image below shows the optical micrograph of the sample after 45° rotation relative to the image above).

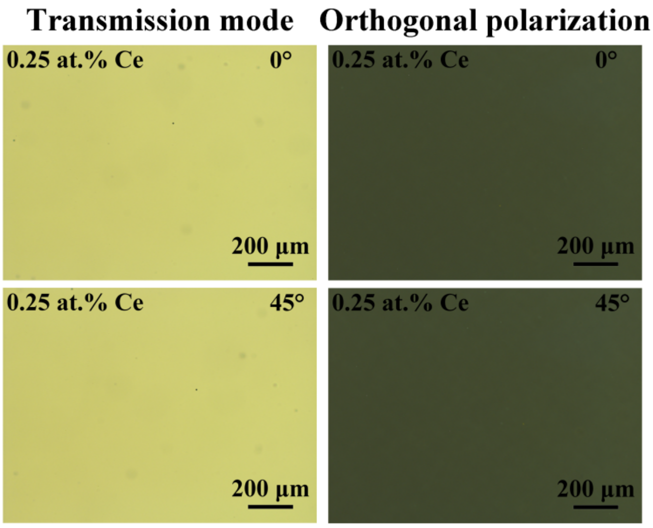

Figure S3. Transmission polarized optical microscopic images of the $Ce_{0.0025}$TSAG ceramic (The image below shows the optical micrograph of the sample after 45° rotation relative to the image above).

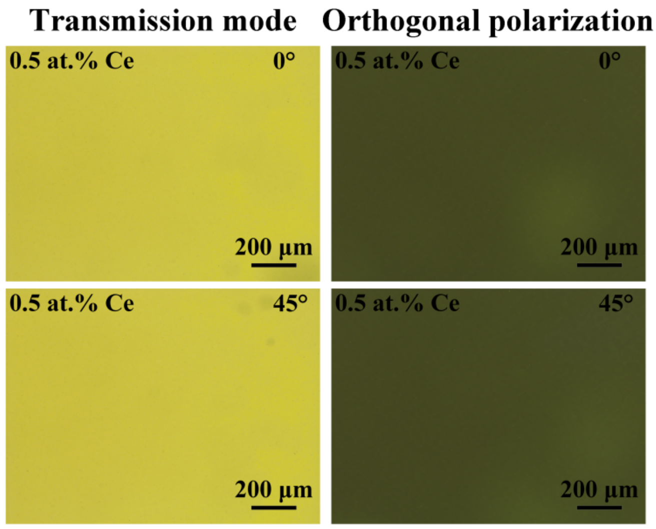

Figure S4. Transmission polarized optical microscopic images of the $Ce_{0.005}TSAG$ ceramic (The image below shows the optical micrograph of the sample after 45° rotation relative to the image above).

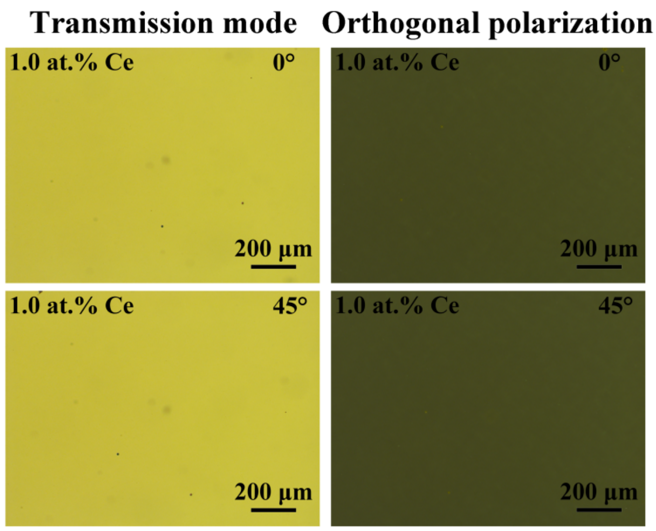

Figure S5. Transmission polarized optical microscopic images of the $Ce_{0.01}TSAG$ ceramic (The image below shows the optical micrograph of the sample after 45° rotation relative to the image above).

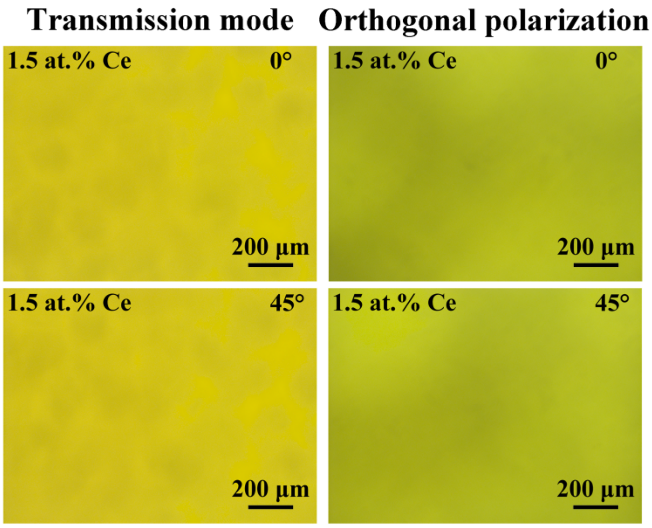

Figure S6. Transmission polarized optical microscopic images of the $Ce_{0.015}TSAG$ ceramic (The image below shows the optical micrograph of the sample after 45° rotation relative to the image above).

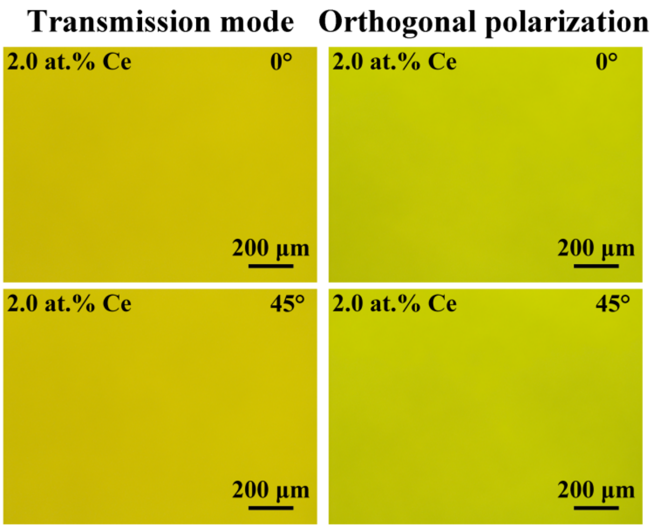

Figure S7. Transmission polarized optical microscopic images of the $Ce_{0.02}TSAG$ ceramic (The image below shows the optical micrograph of the sample after 45° rotation relative to the image above).

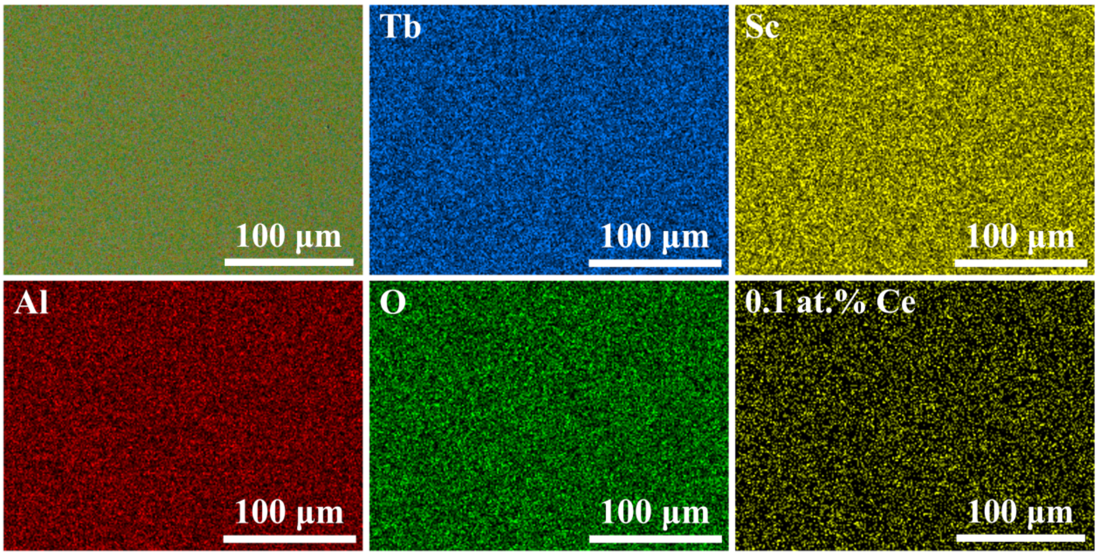

Figure S8. SEM image and EDS mapping results of the $Ce_{0.001}TSAG$ ceramic.

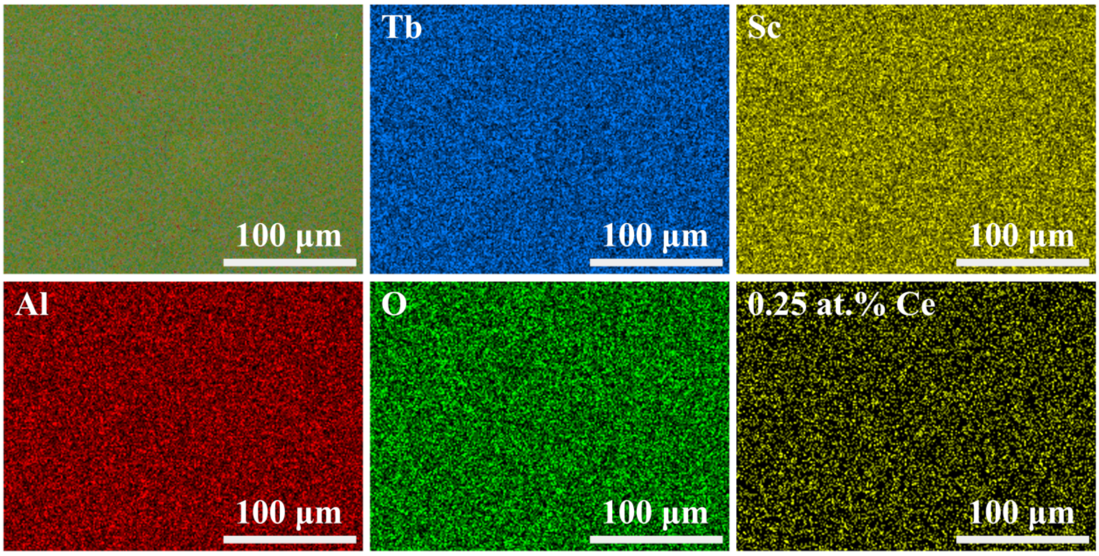

Figure S9. SEM image and EDS mapping results of the $Ce_{0.0025}TSAG$ ceramic.

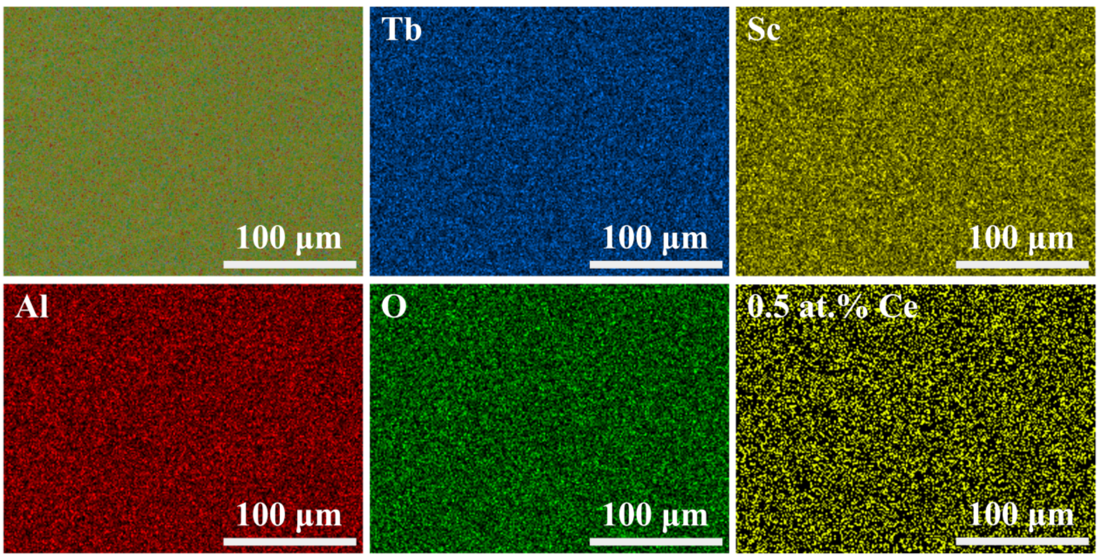

Figure S10. SEM image and EDS mapping results of the $Ce_{0.005}TSAG$ ceramic.

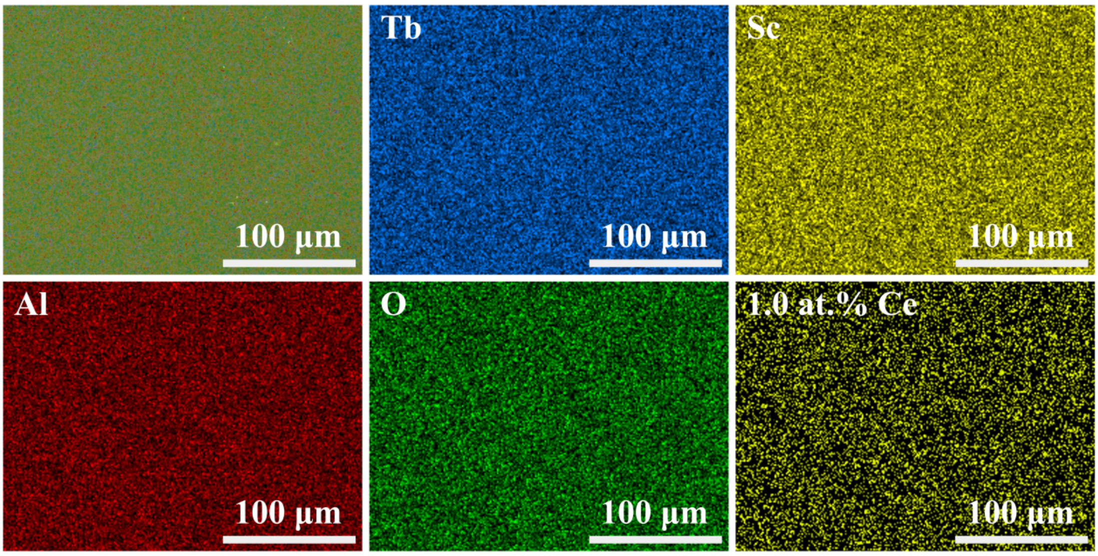

Figure S11. SEM image and EDS mapping results of the $Ce_{0.01}TSAG$ ceramic.

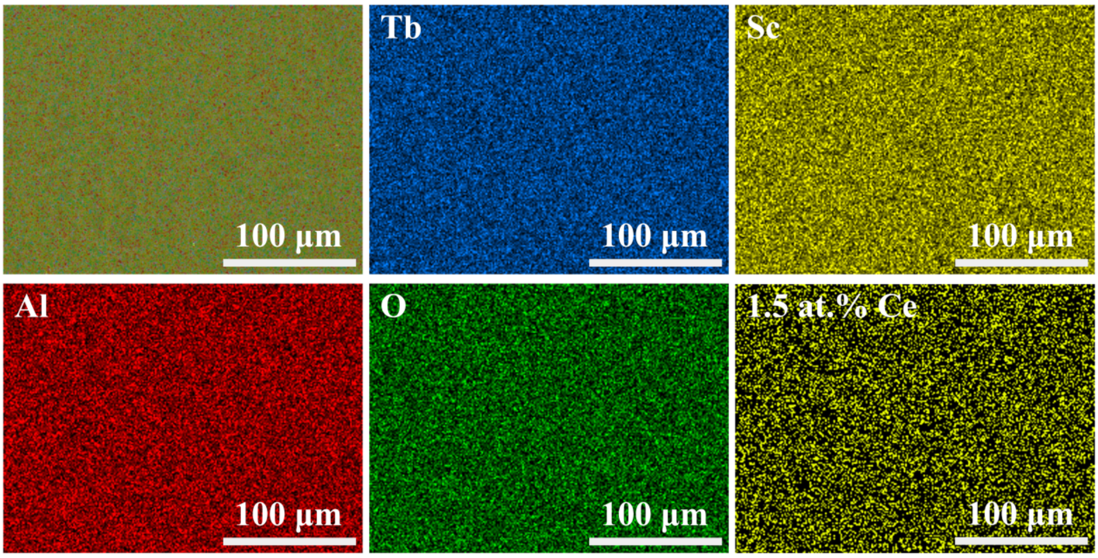

Figure S12. SEM image and EDS mapping results of the $Ce_{0.015}TSAG$ ceramic.

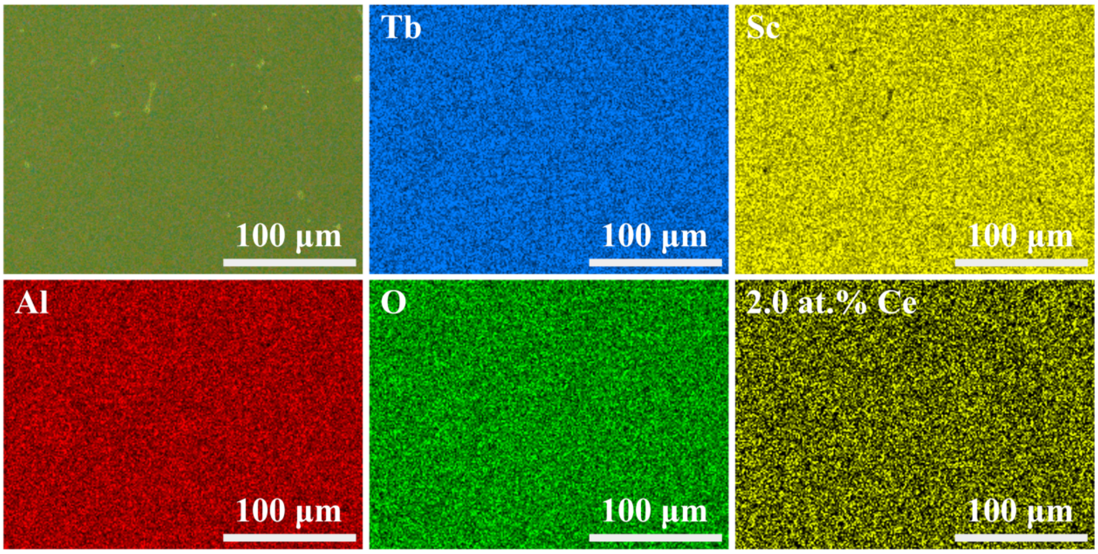

Figure S13. SEM image and EDS mapping results of the $Ce_{0.02}$TSAG ceramic.

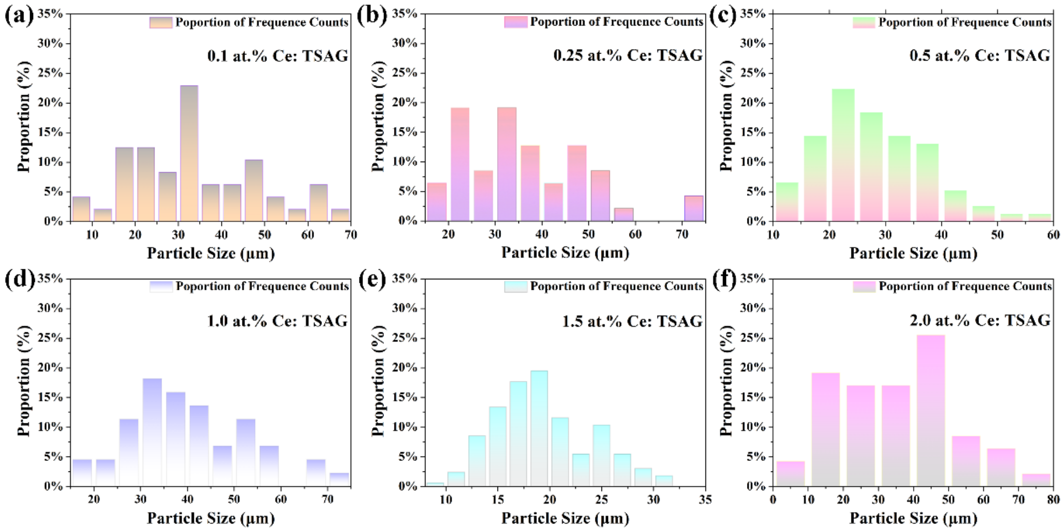

Figure S14. Particle size distribution diagram of (a) $Ce_{0.001}$TSAG ceramic, (b) $Ce_{0.0025}$TSAG ceramic, (c) $Ce_{0.005}$TSAG ceramic, (d) $Ce_{0.01}$TSAG ceramic, (e) $Ce_{0.015}$TSAG ceramic, (f) $Ce_{0.02}$TSAG ceramic. (The units of particle size are μm)

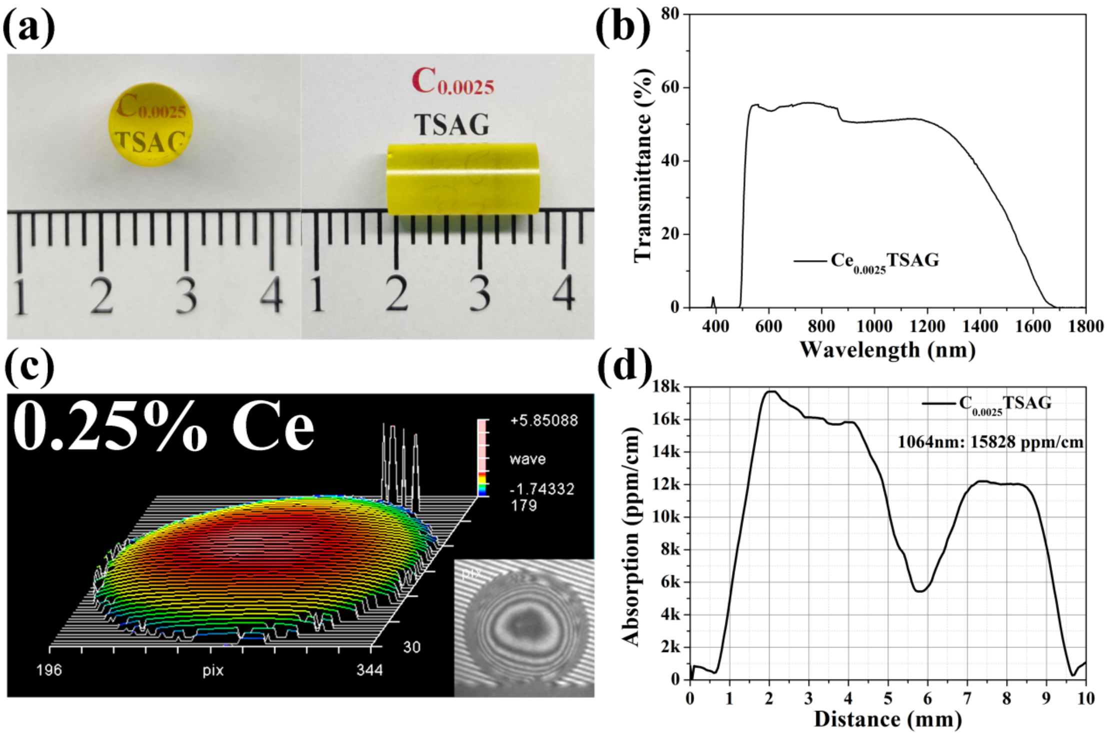

Figure S15. (a) Photograph of the $Ce_{0.0025}$TSAG ceramic (ϕ10 mm × 16 mm). (b) The optical transmittance spectra of the $Ce_{0.0025}$TSAG ceramic. (c) The wave-front intensity map and oblique plot of the $Ce_{0.0025}$TSAG ceramic. (d) The optical weak absorption diagram of the $Ce_{0.0025}$TSAG ceramic.

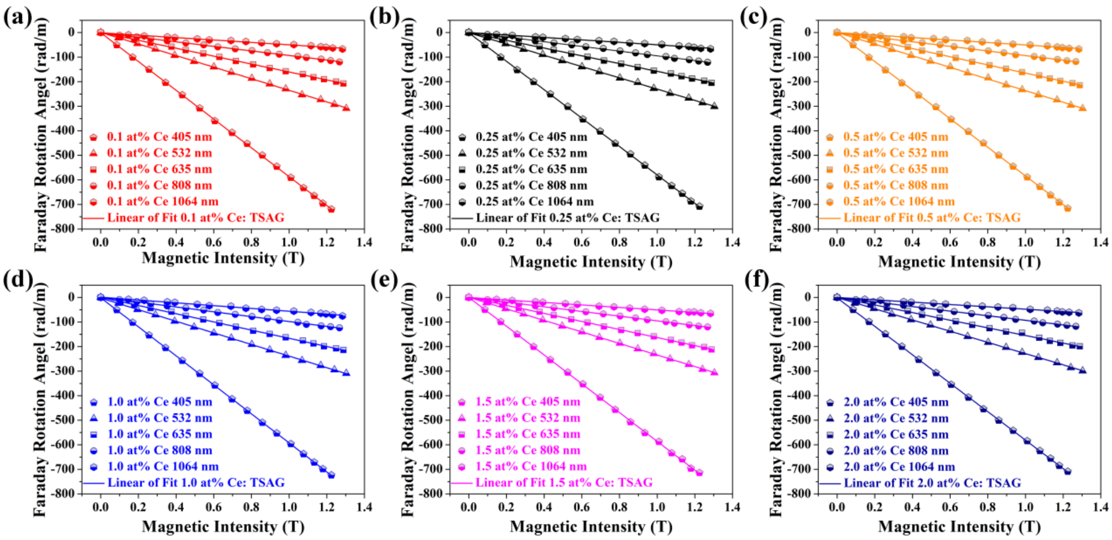

Figure S16. Faraday rotation of (a) $Ce_{0.001}$TSAG ceramic, (b) $Ce_{0.0025}$TSAG ceramic, (c) $Ce_{0.005}$TSAG ceramic, (d) $Ce_{0.01}$TSAG ceramic, (e) $Ce_{0.015}$TSAG ceramic in different wavelengths at room temperature.

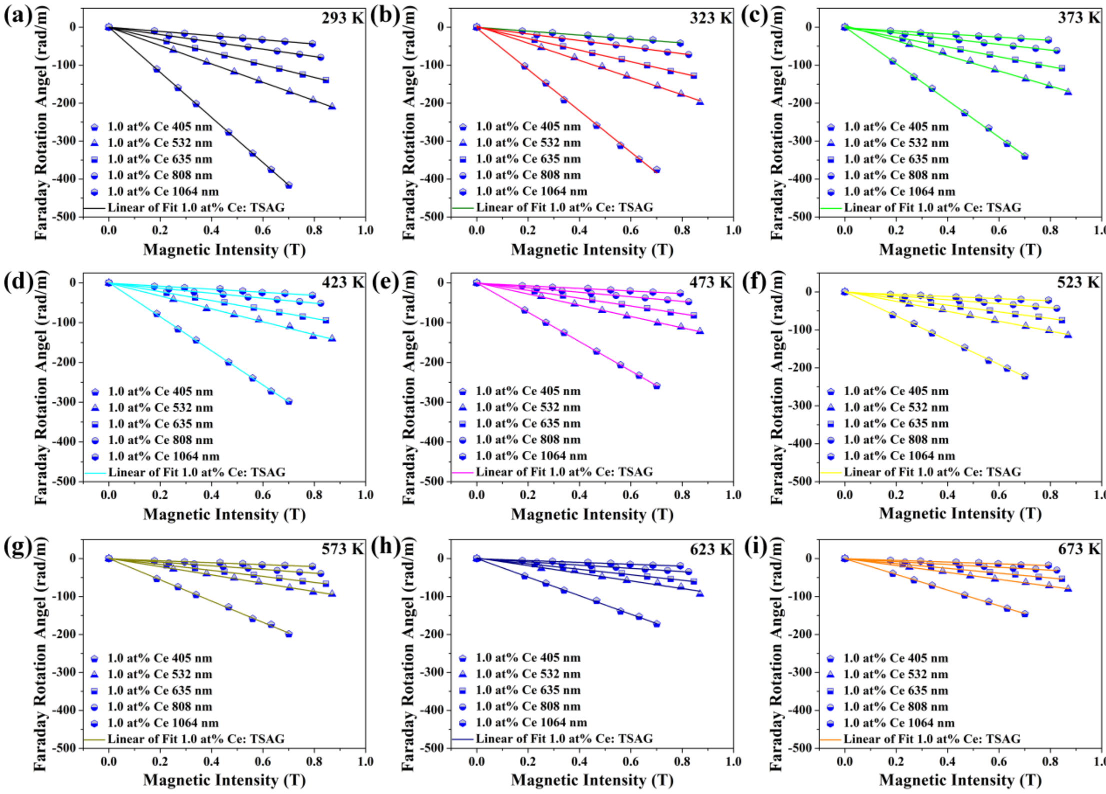

Figure S17. Faraday rotation of $Ce_{0.01}$TSAG in different wavelengths at (a) 293 K, (b) 323 K, (c) 373 K, (d) 423 K, (e) 473 K, (f) 523 K, (g) 573 K, (h) 623 K, (i) 673 K.

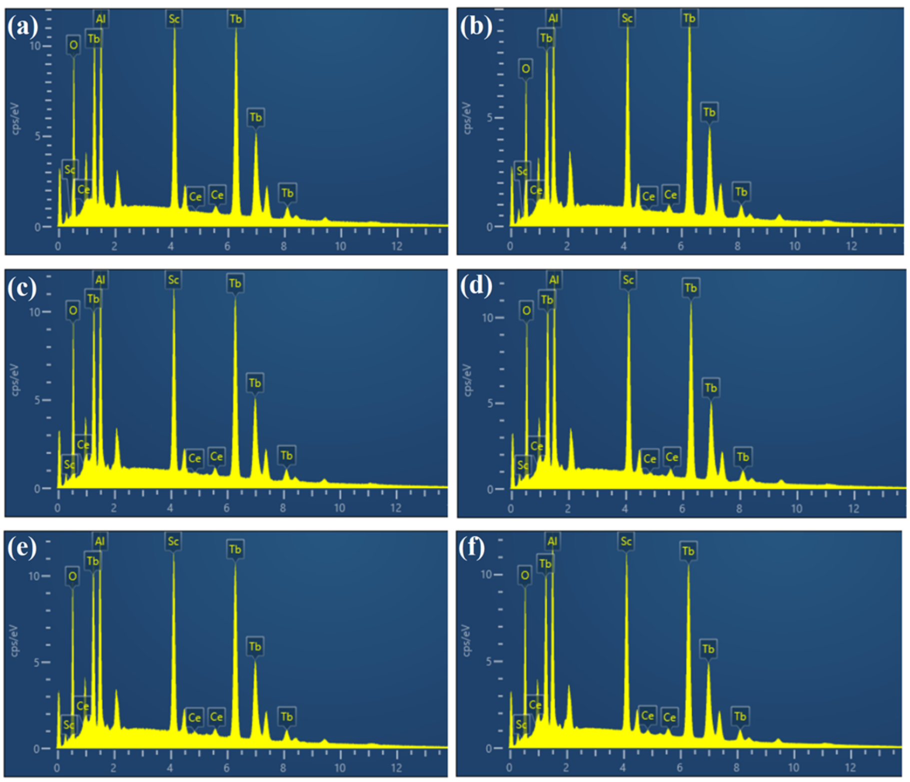

Figure S18. EDS elemental spectrum of $(Tb_{1-x}Ce_x)_3Sc_2Al_3O_{12}$ ceramics (x=0.001, 0.0025, 0.005, 0.01, 0.015, 0.02).

Table S1.

The reliability parameters obtained by XRD Rietveld refinement.

Materials	The reliability parameters	
	Rp	Gof
$Ce_{0.001}$TSAG	8.88%	1.65
$Ce_{0.0025}$TSAG	8.67%	1.49
$Ce_{0.005}$TSAG	7.11%	1.36
$Ce_{0.01}$TSAG	9.56%	1.45
$Ce_{0.015}$TSAG	9.46%	1.60
$Ce_{0.02}$TSAG	7.94%	1.42

Table S2.

Verdet constants of TGG crystal, TSAG ceramic and $(Tb_{1-x}Ce_x)Sc_2Al_3O_{12}$ (x=0.001, 0.0025, 0.005, 0.01, 0.015, 0.02) ceramics at different wavelengths.

Materials	Verdet constant ($rad\cdot m^{-1}\cdot T^{-1}$) at different wavelengths				
	405 nm	532 nm	635nm	808 nm	1064 nm
TGG crystal	-470.2	-190.2	-130.1	-	-40.0
TSAG ceramic	-579.1	-226.1	-150.6	-92.0	-47.8
$Ce_{0.001}$TSAG	-588.4	-234.5	-159.5	-94.5	-51.5
$Ce_{0.0025}$TSAG	-582.6	-231.4	-157.9	-93.2	-49.9
$Ce_{0.005}$TSAG	-586.4	-236.9	-162.9	-94.1	-51.2
$Ce_{0.01}$TSAG	-594.2	-241.6	-165.1	-96.3	-55.0
$Ce_{0.015}$TSAG	-585.6	-233.8	-161.9	-95.0	-50.9
$Ce_{0.02}$TSAG	-582.9	-230.1	-153.9	-92.5	-48.1

Table S3.

Proportionality factor E and transition wavelength λ_0 of $(Tb_{1-x}Ce_x)Sc_2Al_3O_{12}$ (x=0.001, 0.0025, 0.005, 0.01, 0.015, 0.02) ceramics at room temperature.

Materials	Fitted equation: $1/V = 1/E\left(\lambda^2 - \lambda_0^2\right)$	
	Proportionality factor E (10^3 rad·nm^2·T^{-1}·m^{-1})	Transition wavelength λ_0 (nm)
$Ce_{0.001}$TSAG	55286.2	245.5
$Ce_{0.0025}$TSAG	53442.2	256.4
$Ce_{0.005}$TSAG	54776.0	254.2
$Ce_{0.01}$TSAG	59234.3	218.8
$Ce_{0.015}$TSAG	54584.0	254.8
$Ce_{0.02}$TSAG	51398.3	270.2

Table S4.

The temperature-dependent of Verdet constants for the $Ce_{0.01}$TSAG ceramic at different wavelengths.

Temperature	Verdet constant ($rad \cdot m^{-1} \cdot T^{-1}$) at different wavelengths				
	405 nm	532 nm	635nm	808 nm	1064 nm
293 K	-594.2	-241.6	-165.1	-96.3	-55
323 K	-544.4	-226.4	-152.3	-87.0	-51.5
373 K	-483.8	-199.2	-129.0	-75.0	-41.0
423 K	-429.0	-162.1	-112.1	-62.5	-38.5
473 K	-369.1	-141.6	-98.0	-57.3	-32.5
523 K	-318.5	-130.7	-88.3	-52.4	-27.6
573 K	-280.2	-109.4	-79.0	-38.4	-25.4
623 K	-244.6	-100.8	-72.1	-42.6	-24.3
673 K	-206.6	-91.5	-63.0	-37.3	-22.8

Table S5.

Proportionality factor *E* and transition wavelength λ_0 of the $Ce_{0.001}$TSAG ceramic at different temperatures.

$Ce_{0.001}$TSAG	Fitted equation: $1/V = 1/E\left(\lambda^2 - \lambda_0^2\right)$	
	Proportionality factor *E* (10^3 rad • nm^2 • T^{-1} • m^{-1})	Transition wavelength λ_0 (nm)
293 K	59234.3	218.8
323 K	50444.2	258.0
373 K	44753.1	243.1
423 K	39308.5	234.6
473 K	34687.8	230.4
523 K	30287.0	241.8
573 K	27280.7	234.7
623 K	25305.7	215.8
673 K	23055.7	216.3

Table S6

Verdet constants of TSAG ceramics, $(Tb_{1-x}Ce_x)Sc_2Al_3O_{12}$ (x=0.001, 0.0025, 0.005, 0.01, 0.015, 0.02) ceramics, TSAG crystals, and TGG crystals at different wavelengths.

Materials	Verdet constant ($rad\cdot m^{-1}\cdot T^{-1}$) at different wavelengths				
	405 nm	532 nm	635nm	808 nm	1064 nm
TSAG ceramic	-579.1	-226.1	-150.6	-92.0	-47.8
$Ce_{0.001}$TSAG	-588.4	-234.5	-159.5	-94.5	-51.5
$Ce_{0.0025}$TSAG	-582.6	-231.4	-157.9	-93.2	-49.9
$Ce_{0.005}$TSAG	-586.4	-236.9	-162.9	-94.1	-51.2
$Ce_{0.01}$TSAG	-594.2	-241.6	-165.1	-96.3	-55.0
$Ce_{0.015}$TSAG	-585.6	-233.8	-161.9	-95.0	-50.9
$Ce_{0.02}$TSAG	-582.9	-230.1	-153.9	-92.5	-48.1
TSAG crystal[1]	-	-218.0	-152@633 nm	-	-65.0
TGG crystal	-470.2	-190.2	-130.1	-	-40.0

References

[1] R. Q. Dou, H. T. Zhang, Q. L. Zhang, N. F. Zhuang, W. P. Liu, Y. He, Y. Y. Chen, M. J. Cheng, J. Q. Luo and D. L. Sun, Growth and properties of TSAG and TSLAG magneto-optical crystals with large size, *Opt. Mater.*, 2019, **96**, 109272.